Influence of Macrocyclic Ring Size on the Corrosion Inhibition Efficiency of Dibenzo Crown Ether: A Density Functional Study

Saprizal Hadisaputra[1,*], Saprini Hamdiani[1], Muhammad Arsyik Kurniawan[2], and Nuryono[3]

[1]*Department of Chemistry Education, Faculty of Science and Education, University of Mataram, Jl. Majapahit No 62, Mataram, 83125, Indonesia*

[2]*Department of Chemistry, Faculty of Mathematics and Natural Science, Universitas Islam Indonesia, Jl. Kaliurang KM 14.5, Yogyakarta 55584, Indonesia*

[3]*Department of Chemistry, Faculty of Mathematics and Natural Sciences, Universitas Gadjah Mada, Sekip Utara, Yogyakarta 55281, Indonesia*

Received July 18, 2017; Accepted September 4, 2017

ABSTRACT

The effect of macrocycle ring size on the corrosion inhibition efficiency of dibenzo-12-crown-4 (DB12C4), dibenzo-15-crown-5 (DB15C5), dibenzo-18-crown-6 (DB18C6), dibenzo-21-crown-7 (DB21C7) and dibenzo-24-crown-8 (DB24C8) have been elucidated by mean of density functional calculation at B3LYP/6-31G(d) level of theory in the gas and aqueous environment. The quantum chemical parameters including the frontier orbital energies (E_{HOMO}, E_{LUMO}), ionization potential (I), electron affinity (A), the absolute electronegativity (χ), hardness (η), softness (σ), and the fraction of electron transferred (ΔN) are positively correlated to the corrosion inhibition efficiency (IE%) of the studied crown ethers. The calculation results indicate that DB24C8 exhibits the highest corrosion inhibition efficiency, whereas DB12C4 exhibits the lowest corrosion inhibition efficiency. The results of this study will contribute to design crown ethers potential as corrosion inhibitors.

Keywords: *crown ether; corrosion inhibition; ring size; DFT method*

ABSTRAK

Pengaruh ukuran cincin makrosiklik terhadap efisiensi inhibitor korosi senyawa dibenzo-12-mahkota-4 (DB12C4), dibenzo-15-mahkota-5 (DB15C5), dibenzo-18-mahkota-6 (DB18C6), dibenzo-21-mahkota-7 (DB21C7) and dibenzo-24-mahkota-8 (DB24C8) pada fasa gas dan larutan telah dihitung menggunakan teori fungsional kerapatan pada tingkatan teori B3LYP/6-31G(d). Parameter kimia kuantum seperti orbital energi (E_{HOMO}, E_{LUMO}), potensial ionisasi (I), afinitas elektron (A), elektronegativitas mutlak (χ), sifat keras (η), sifat lunak (σ) dan jumlah transfer elektron (ΔN) berkorelasi positif dengan efisiensi inhibitor korosi (IE%) dari senyawa dibenzo eter mahkota. Hasil perhitungan menunjukkan bahwa DB24C8 memiliki efisiensi inhibitor korosi tertinggi sedangkan DB12C4 memiliki efisiensi inhibitor korosi terendah. Hasil kajian ini akan berkontribusi besar pada proses desain senyawa eter mahkota yang potensial sebagai inhibitor korosi.

Kata Kunci: *eter mahkota; inhibitor korosi; ukuran cincin; Metode DFT*

INTRODUCTION

Corrosion is an inevitable electrochemical process for less noble metals and alloys. It gradually destroys metallic structures when metals interact with a corrosive environment such as hydrochloric acid [1]. Having no prevention, corrosion processes may lead to massive economic losses. Therefore, intensive efforts to gain high-efficiency and the feasible use of the corrosion inhibitors still a very active research area. Moreover, searching for less toxic and environment-friendly corrosion inhibitors becomes significantly important due to the increased awareness of the importance of the green chemistry applications. A variety of organic compounds has been used as green corrosion inhibitor [2-8]. Most the efficient organic inhibitors contain electronegative functional groups in which incorporate heteroatoms such as oxygen, nitrogen, sulfur, phosphorus (O, N, S, and P) and π-electron in multiple bonds [9-11]. These types of functional groups facilitate the formation of complexes between organic inhibitors and metal surfaces via a coordinate covalent bond (chemical adsorption) or an electrostatic interaction (physical adsorption) [12]. The complex formation

* Corresponding author.
Email address : rizal@unram.ac.id

DOI: 10.22146/ijc.26667

between organic inhibitors and metal surfaces creates a uniform film on the metal surface, which prevents contact with the corrosive medium [13].

A major research effort on the metallic corrosion inhibition properties of many organic inhibitors has been devoted. However, very few experimental studies have been attempted to study the role of crown ethers as an organic corrosion inhibitor. Crown ethers have received increasing interest since they were first characterized by Pedersen [14-15]. Their ability to selectively bind metal ions has led to a wide range of applications such as sensing [13], phase-transfer catalysis [16], extraction [17] and corrosion inhibitor as currently reported [18-19]. The properties of crown ethers can easily be tuned by modifying their heteroatom (O, N, S, and P), and adding the π-electron in multiple bonds such as benzene groups to meet the criteria of corrosion inhibitor. Furthermore, crown ethers are less toxic and environment-friendly which are suitable for green corrosion inhibitors. Fouda et al. [19] reported that crown ethers are highly potential candidate for corrosion inhibitor and they show good corrosion inhibitor efficiencies.

The quantum chemical investigation has been used extensively to study the interaction of crown ether with some metal ions. These studies have been performed on the effect of macrocyclic ring size, donor atoms, electron donating and withdrawing substitution on the metal ion-crown ether interaction [20-23]. The quantum chemical approach also has been used to investigate the corrosion inhibitor of many organic inhibitors [24-28]. In this current work, we use the quantum chemical investigation to study the effect of macrocyclic ring size on the corrosion inhibition efficiency of dibenzo-crown ethers.

COMPUTATIONAL METHOD

The geometries of crown ether were determined using Density functional theory (DFT) in the hybrid B3LYP [29-31]. All calculations including the quantum chemical parameters were performed using the Gaussian 03 package [32]. In order to reach the ground state geometry, no symmetry constraint was applied during geometry optimization. The quantum chemical parameters such as the energy of the highest occupied molecular orbital (E_{HOMO}), the energy of the lowest unoccupied molecular orbital (E_{LUMO}), the ionization potential (I), the electron affinity (*A*), the absolute electronegativity (χ), hardness (η), softness (σ), the fraction of electron transferred (ΔN), and the corrosion inhibitors (IE%) efficiencies were calculated.

According to Koopman's theorem [33], ionization potential (I) and electron affinity (A), the electronegativity (χ) and global hardness (η) may be defined in terms of the energy of the HOMO and the LUMO. Ionization potential (I) is defined as the amount of energy required to remove an electron from a molecule [34]. It is related to the energy of the E_{HOMO} through the eq. 1:

$$I = -E_{HOMO} \quad (1)$$

Electron affinity (A) is defined as the energy released when a proton is added to a system [34]. It is related to E_{LUMO} through the eq. 2:

$$A = -E_{LUMO} \quad (2)$$

The electronegativity is the measure of the power of an atom or group of atoms to attract electrons towards itself [35], it can be estimated by using the eq. 3:

$$\chi = \frac{I + A}{2} \quad (3)$$

Chemical hardness (η) measures the resistance of an atom to a charge transfer [35], it is estimated by using the eq. 4:

$$\eta = \frac{I - A}{2} \quad (4)$$

According to Pearson theory [36] the fraction of transferred electrons (ΔN) from the inhibitor molecule to the metallic atom can be calculated (eq. 5):

$$\Delta N = \frac{\chi Fe - \chi Inh}{2(\eta Fe + \eta inh)\pi r^2} \quad (5)$$

where χFe and χinh denote the absolute electronegativity of iron and inhibitor molecule respectively ηFe and ηin denote the absolute hardness of iron and the inhibitor molecule, respectively. In order to calculate the fraction of electrons transferred, the theoretical value for the electronegativity of bulk iron was used χFe = 7.0 eV [37] and a global hardness of ηFe = 0 by assuming that for a metallic bulk I = A [38].

In order to investigate the correlation of the quantum chemical parameters with the corrosion inhibitor performance of crown ether, the inhibition efficiencies for dibenzo crown ether models have been determined using eq. 6-8 [39]:

$$I_{add}\% = \frac{I_{CE} - I_{x-CE}}{I_{CE}} \times 100\% \quad (6)$$

$$IE_{add}.\% = I_{add}.\% - I_{eCe}.\% \quad (7)$$

$$IE_{theor}.\% = I_{eCe}.\% + IE_{add}.\% \quad (8)$$

where $I_{add}.\%$ is the percentage ionization potential of the dibenzo crown ether, $IE_{add}.\%$ is the inhibition efficiency % of the dibenzo crown ether, and $IE_{theor}.\%$ is the theoretically calculated percentage inhibition efficiency. The practical experimented values of the inhibition efficiency of dibenzo-24-crown-8 and dibenzo-18-crown-6 were 82.02 and 63.13%, respectively [19].

The solvent effects are included using the polarized continuum model (PCM) as implemented in the Gaussian code due to corrosion dominantly occurred in aqueous environment. The dielectric

constant for the water solvent was taken as 78.4. In employing PCM model, the single-point calculations on gas-phase geometries are sufficient for energetic. Structure re-optimization in the presence of the solvent was found to have a minor influence on energetic [20-21,23].

RESULT AND DISCUSSION

Five dibenzo crown ether derivatives with different ring sizes were investigated as depicted in Scheme 1. Fig. 1 shows the structure of the optimized geometries of (DB12C4), dibenzo-15-crown-5 (DB15C5), dibenzo-18-crown-6 (DB18C6), dibenzo-21-crown-7 (DB21C7) and dibenzo-24-crown-8 (DB24C8) calculated with DFT B3LYP/6-31G(d) level of theory. The presence of benzene ring making the molecule rigid and it leads to a small number of conformational isomers as a result, the computational effort was also reduced. The structure optimization was conducted by Cs conformation.

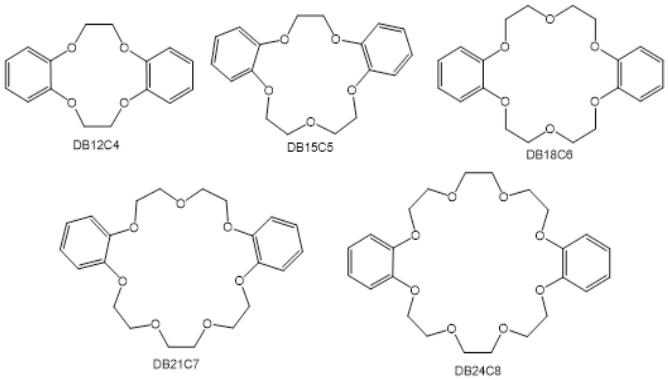

Scheme 1. Molecular structures of the studied molecules

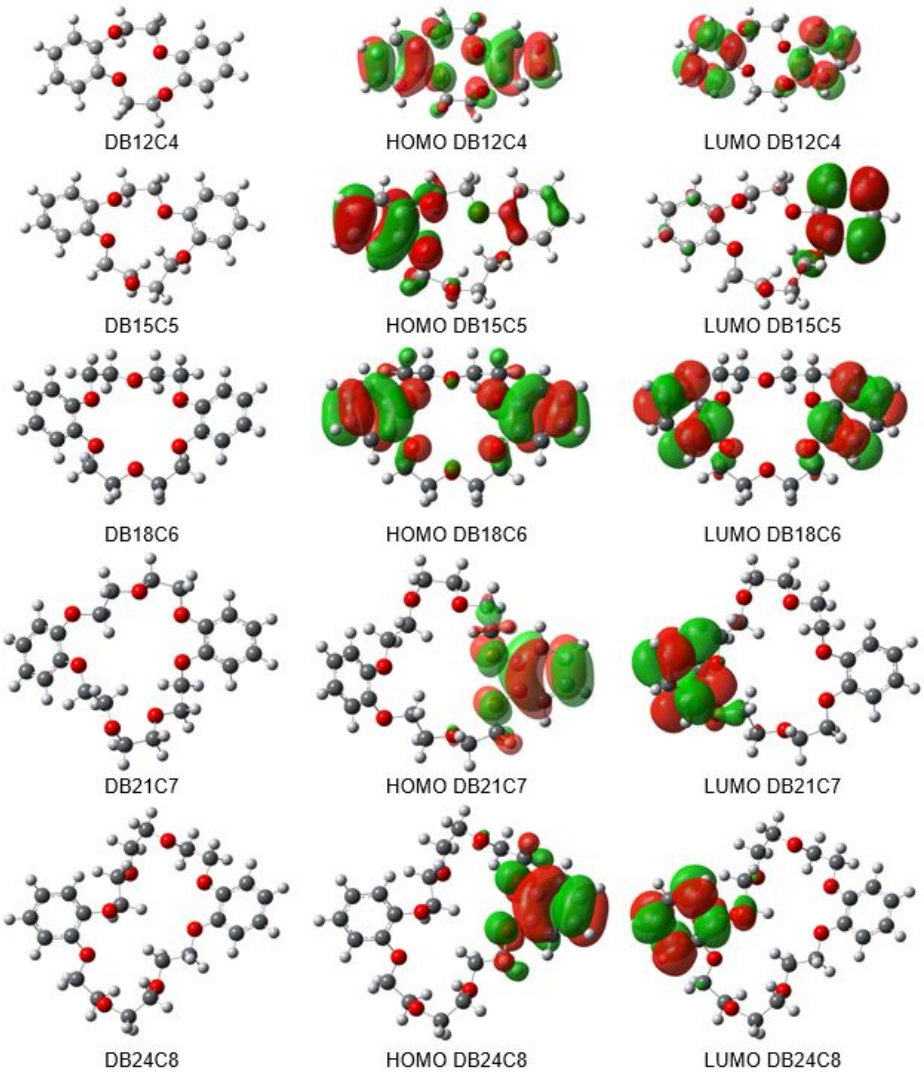

Fig 1. The optimized structures and HOMO-LUMO orbitals of the studied free molecules determined using DFT method at the B3LYP/6-31G(d) level of theory

Table 1. Quantum-chemical parameters for five models of dibenzo crown ether determined using DFT method at the B3LYP/6-31G(d) level of theory at gas (G) and solvent (W) phase

Compounds		E_{HOMO} (eV)	E_{LUMO} (eV)	E_{gab} (eV)	*I* (eV)	*A* (eV)	χ (eV)	η (eV)	σ (eV)	ΔN	$IE_{theor.}$%
DB24C8	G	-5.3789	0.1972	5.5762	5.3789	-0.1973	2.5908	2.7881	0.3587	0.7907	82.0200
	W	-5.6117	0.0144	5.6262	5.6117	-0.0144	2.7987	2.8131	0.3555	0.7467	78.4692
DB21C7	G	-5.4594	0.2318	5.6913	5.4594	-0.2318	2.6138	2.8456	0.3514	0.7706	80.7918
	W	-5.6007	0.0212	5.6219	5.6007	-0.0212	2.7897	2.8109	0.3558	0.7489	78.6383
DB18C6	G	-5.5805	0.2242	5.8047	5.5805	-0.2242	2.6781	2.9024	0.3445	0.7445	63.1300
	W	-5.8793	-0.0299	5.8494	5.8793	0.0299	2.9546	2.9247	0.3419	0.6915	59.7500
DB15C5	G	-5.7064	0.1151	5.8215	5.7064	-0.1151	2.7957	2.9108	0.3436	0.7222	61.7054
	W	-5.843	0.0307	5.8738	5.843	-0.0308	2.9061	2.9369	0.3405	0.6969	58.7355
DB12C4	G	-5.6526	0.1994	5.852	5.6526	-0.1995	2.7265	2.926	0.3418	0.7302	60.8904
	W	-5.7862	0.0775	5.8637	5.7862	-0.0776	2.8543	2.9319	0.3411	0.7070	58.5639

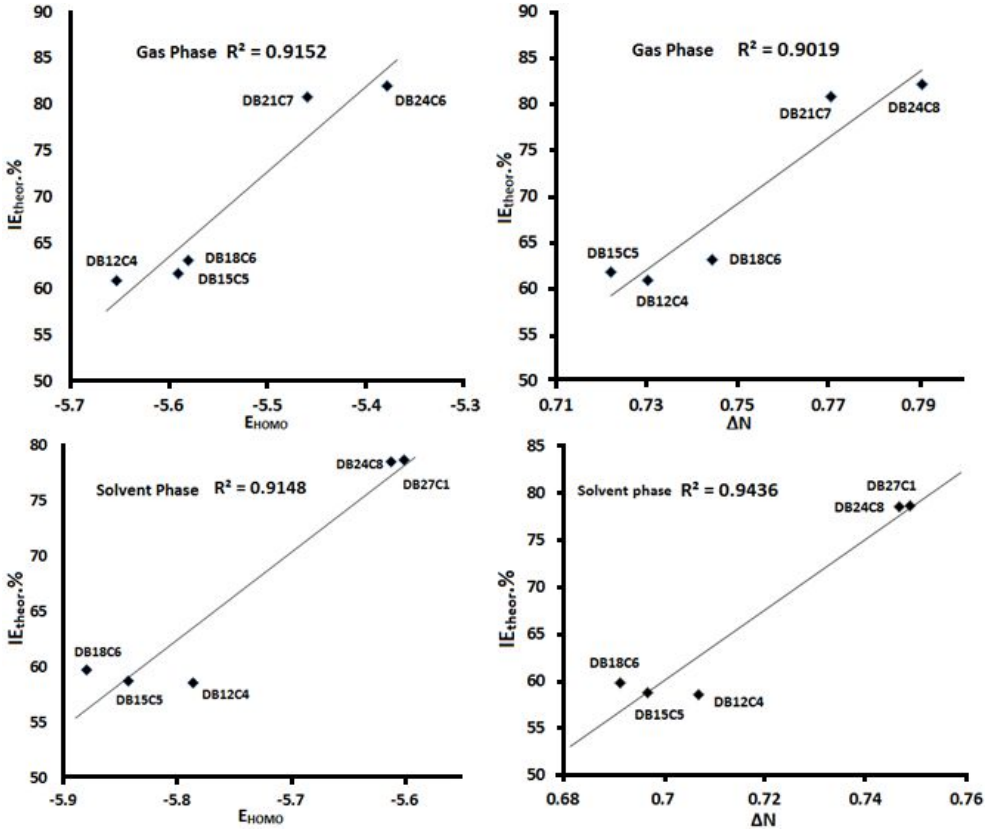

Fig 2. Correlation between E_{HOMO} and the number of electrons transferred (ΔN) with corrosion inhibition efficiency (IE%) of five models of dibenzo crown ether in gas and solvent phase

The frontier molecular orbitals related to the reactivity of the dibenzo-crown ethers are reported in Table 1. The interaction between E_{HOMO} and E_{LUMO} of reacting species lead to the transition of electrons within molecules [40]. The transition of electron includes donation and acceptation of electron is measured by the energy value of molecular orbitals. The HOMO energy indicates the tendency of molecule towards the donation of electrons. It is found that dibenzo crown ethers with larger macrocycle ring size have higher HOMO energies than those with smaller macrocycle ring size. Therefore, they are more intent to donating electrons than smaller macrocycle ring sizes are. It can be seen that the E_{HOMO} for the dibenzo crown ether models follow the order of DB24C8 > DB21C7 > DB18C6 > DB15C5 > DB12C4. This trend can be used as a preliminary prediction that DB24C8 will have the highest corrosion inhibitor efficiency.

Fig. 1 shows the frontier molecular orbital visualization of DB12C4, DB15C5, DB18C6, DB21C7 and DB24C8 calculated by B3LYP/6-31G(d) level of theory. It indicates that the HOMO of these crown ether

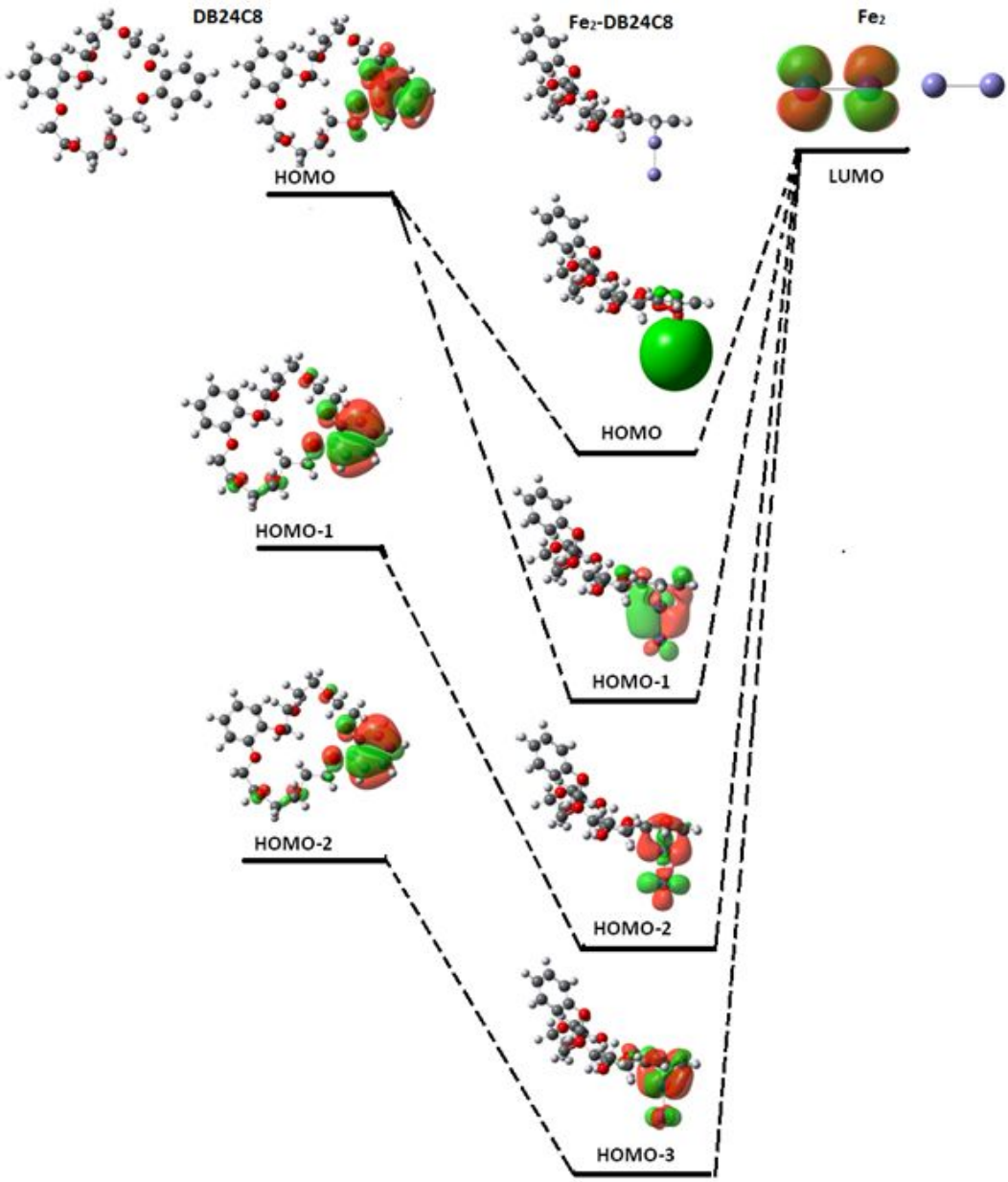

Fig 3. Interaction of molecular orbital DB24C8 with Fe_2 cluster

compounds matches with the aromatic π system of the benzene rings in which the electron density accumulates on the π-electron multiple bonds of benzene. Apparently, it is expected that the enhancement of the π-electron due to macrocycle ring size in benzene contributes for interacting with metal surfaces. The phenyl rings of dibenzo crown ether have higher binding contribution to metal surfaces via delocalization of π-electron.

The number of electrons transferred (ΔN) was also presented in Table 1. The inhibition efficiency increases by increasing of macrocycle ring size of these inhibitors to donate electrons to the metal surface. The results indicate that ΔN values strongly correlate with the experimental and predicted inhibition efficiencies. Thus, the highest fraction of electrons transferred is associated with the best inhibitor DB24C8, whereas the least fraction is associated with the inhibitor that has the least inhibition efficiency. The correlation between the electrons transferred and inhibition efficiencies in gas and aqueous phase is depicted in Fig. 2. A linear correlation has been identified between electrons transferred and inhibition efficiencies in gas r^2 = 0.9148 and aqueous phase r^2 = 0.9436. A linear correlation also has been identified between HOMO energies and inhibition efficiencies in gas and aqueous phase, r^2 = 0.9152 and r^2 = 0.9148, respectively.

In order to investigate the correlation of the quantum chemical parameters with the corrosion inhibitor performance of crown ether, the calculated inhibition efficiencies for dibenzo crown ether models have been determined using the previously reported formula by Obayes et al. [40]. The calculated and practical experimented inhibition efficiency values are depicted in Table 1. The corrosion inhibition efficiency data shows that the presence of larger macrocycle ring size on the framework of dibenzo crown ether increases inhibition efficiency by approximately 18.89%, from DB18C6 to DB24C8. In contrast, the smaller macrocycle ring size reduces the inhibition efficiency by 3.1%, from DB18C6 to DB12C4. Therefore, the lowest inhibition efficiency is DB12C4 and the highest inhibition efficiency is DB24C8.

In order to understand the molecular level adsorption of corrosion inhibitor over the metal surface, the molecular interaction of DB24C8 with Fe_2 cluster was studied. The geometry optimization of Fe_2-DB24C8 was performed in the ground electronic state. The ground electronic state is the state in which the inhibitor most likely exists during the bond formation between the inhibitor and the metal surface [44]. Interaction of molecular orbital DB24C8 with Fe_2 cluster was depicted in Fig. 3. It showed that the delocalization from aromatic benzene ring assists to a greater extent in giving up its π electron density through its HOMO orbital to metal LUMO orbital. This π electron density transfer leads to DB24C8 adsorption over the Fe_2 cluster. It indicated that the HOMO-LUMO orbitals involve in adsorption reaction with the Fe_2 cluster. Moreover, it is found that the HOMO-1 orbital of DB24C8 also has the capacity to transfer the electron clouds toward the Fe_2 cluster. This adsorption mechanism is consistent with previous studies [44-47] that the HOMO orbitals of the aromatic system strongly interact with the metallic orbitals through the chemisorption reaction [48].

CONCLUSION

Quantum chemical parameters including the energy of the highest occupied molecular orbital (E_{HOMO}) and the lowest unoccupied molecular orbital (E_{LUMO}), ionization potential (I), electron affinity (A), the absolute electronegativity (χ), hardness (η), softness (σ), the fraction of electron transferred (ΔN), and the inhibitors efficiencies dibenzo crown ether have been studied by B3LYP/6-31G(d) level of theory. To the system under consideration, the calculation results indicated that the highest occupied molecular orbital E_{HOMO} and the fraction of electron transferred (ΔN) have a good correlation with the corrosion inhibition efficiency (IE%). Larger macrocycle ring size increases the inhibition efficiency, in contrast, smaller macrocycle ring size has the opposite effect. It is found that DB24C8 exhibits the highest inhibition efficiency, whereas DB12C4 exhibits the lowest highest inhibition efficiency.

ACKNOWLEDGEMENT

Financially supported from *Hibah Penelitian Pascadoktor RISTEKDIKTI* Indonesia 2017 is gratefully acknowledged.

REFERENCES

[1] Uhlig, H.H., and Revie, R.W., 1985, Corrosion and Corrosion Control: An Introduction to Corrosion Science and Engineering, John Wiley & Sons, inc., America, 1–7.

[2] Qiang, Y., Zhang, S., Guo, L., Xu, S., Feng, L., Obot, I.B., and Chen, S., 2017, Sodium dodecyl benzene sulfonate as a sustainable inhibitor for zinc corrosion in 26% NH_4Cl solution, *J. Cleaner Prod.*, 152, 17–25.

[3] Mobin, M., and Rizvi, M., 2017, Polysaccharide from *Plantago* as a green corrosion inhibitor for carbon steel in 1 M HCl solution, *Carbohydr. Polym.*, 160, 172–183.

[4] Douadi, T., Hamani, H., Daoud, D., Al-Noaimi, M., and Chafaa, S., 2017, Effect of temperature and hydrodynamic conditions on corrosion inhibition of an azomethine compounds for mild steel in 1 M HCl solution, *J. Taiwan Inst. Chem. Eng.*, 71, 388–404.

[5] Zarrouk, A., Hammouti, B., Lakhlifi, T., Traisnel, M., Vezin, H., and Bentiss, F., 2015, New 1*H*-pyrrole-2,5-dione derivatives as efficient organic inhibitors of carbon steel corrosion in hydrochloric acid medium: Electrochemical, XPS and DFT studies, *Corros. Sci.*, 90, 572–584.

[6] Yıldız, R., Döner, A., Doğan, T., and Dehri, İ., 2014, Experimental studies of 2-pyridinecarbonitrile as corrosion inhibitor for mild steel in hydrochloric acid solution, *Corros. Sci.*, 82, 125–132.

[7] Mendonça, G.L.F., Costa, S.N., Freire, V.N., Casciano, P.N.S., Correia, A.N., and Lima-Neto, P.D., 2017, Understanding the corrosion inhibition of carbon steel and copper in sulphuric acid medium by amino acids using electrochemical techniques allied to molecular modelling methods, *Corros. Sci.,* 115, 41–55.

[8] Noor, E.A., 2005, The inhibition of mild steel corrosion in phosphoric acid solutions by some N-heterocyclic compounds in the salt form, *Corros. Sci.*, 47 (1), 33–55.

[9] Purwoko, A.A., and Hadisaputra, S., 2017, Experimental and theoretical study of the

substituted (H^6-arene)$Cr(CO)_3$ complexes, *Orient. J. Chem.*, 33 (2), 717–724.

[10] Shetty, S.K., and Shetty, A.N., 2017, Eco-friendly benzimidazolium based ionic liquid as a corrosion inhibitor for aluminum alloy composite in acidic media, *J. Mol. Liq*., 225, 426–438.

[11] Benabid, S., Douadi, T., Issaadi, S., Penverne, C., and Chafaa, S., 2017, Electrochemical and DFT studies of a new synthesized Schiff base as corrosion inhibitor in 1 M HCl, *Measurement*, 99, 53–63.

[12] Salarvand, Z., Amirnasr, M., Talebian, M., Raeissi, K., and Meghdadi, S., 2017, Enhanced corrosion resistance of mild steel in 1M HCl solution by trace amount of 2-phenyl-benzothiazole derivatives: Experimental, quantum chemical calculations and molecular dynamics (MD) simulation studies, *Corros. Sci*., 114, 133–145.

[13] Wang, Y., and Zuo, Y., 2017, The adsorption and inhibition behavior of two organic inhibitors for carbon steel in simulated concrete pore solution, *Corros. Sci*., 118, 24–30.

[14] Pedersen, C.J., 1970, Crystalline salt complexes of macrocyclic polyethers, *J. Am. Chem. Soc.*, 92 (2), 386–391.

[15] Pedersen, C.J., 1967, Cyclic polyethers and their complexes with metal salts, *J. Am. Chem. Soc*., 89 (26), 2495–2496.

[16] Du, J., Huang, Z., Yu, X.Q., and Pu, L., 2013, Highly selective fluorescent recognition of histidine by a crown ether–terpyridine–Zn(II) sensor, *Chem. Commun*., 49 (47), 5399–5401.

[17] Hong, M., Wang, X., You, W., Zhuang, Z., and Yu, Y., 2017, Adsorbents based on crown ether functionalized composite mesoporous silica for selective extraction of trace silver, *Chem. Eng. J*., 313, 1278–1287.

[18] Hasanov, R., Bilge, S., Bilgiç, S., Gece, G., and Kılıç, Z., 2010, Experimental and theoretical calculations on corrosion inhibition of steel in 1 M H_2SO_4 by crown type polyethers, *Corros. Sci.,* 52 (3), 984–990.

[19] Fouda, A.S., Abdallah, M., Al-Ashrey, S.M., and Abdel-Fattah, A.A., 2010, Some crown ethers as inhibitors for corrosion of stainless steel type 430 in aqueous solutions, *Desalination*, 250 (2), 538–543.

[20] Hadisaputra, S., Canaval, L.R., Pranowo, H.D., and Armunanto, R., 2014, Theoretical study of substituent effects on Cs^+/Sr^{2+}–dibenzo-18-crown-6 complexes, *Monatsh. Chem.*, 145 (5), 737–745.

[21] Hadisaputra, S., Canaval, L.R., Pranowo, H.D., and Armunanto, R., 2014, Theoretical study on the extraction of alkaline earth salts by 18-crown-6: Roles of counterions, solvent types and extraction temperatures, *Indones. J. Chem.*, 14 (2), 199–208.

[22] Canaval, L.R., Hadisaputra, S., and Hofer, T.S., 2015, Remarkable conformational flexibility of aqueous 18-crown-6 and its strontium(II) complex – *ab initio* molecular dynamics simulations, *Phys. Chem. Chem. Phys*., 17 (25), 16359–16366.

[23] Hadisaputra, S., Pranowo, H.D., and Armunanto, R., 2012, Extraction of strontium(II) by crown ether: Insights from density functional calculation, *Indones. J. Chem*., 12 (3), 207–216.

[24] Kaya, S., Lei, G., Kaya, C., Tüzün, B., Obot, I.B., Touir, R., and Islam, N., 2016, Quantum chemical and molecular dynamic simulation studies for the prediction of inhibition efficiencies of some piperidine derivatives on the corrosion of iron, *J. Taiwan Inst. Chem. Eng*., 65, 522–529.

[25] Zarrouk, A., El Ouali, I., Bouachrine, M., Hammouti, B., Ramli, Y., Essassi, E.M., and Salghi, R., 2013, Theoretical approach to the corrosion inhibition efficiency of some quinoxaline derivatives of steel in acid media using the DFT method, *Res. Chem. Intermed*., 39 (3), 1125–1133.

[26] Obot, I.B., Kaya, S., Kaya, C., and Tüzün, B., 2016, Theoretical evaluation of triazine derivatives as steel corrosion inhibitors: DFT and Monte Carlo simulation approaches, *Res. Chem. Intermed*., 42 (5), 4963–4983.

[27] Zhang, D., Tang, Y., Qi, S., Dong, D., Cang, H., and Lu, G., 2016, The inhibition performance of long-chain alkyl-substituted benzimidazole derivatives for corrosion of mild steel in HCl, *Corros. Sci.,* 102, 517–522.

[28] Saha, S.K., Hens, A., Murmu, N.C., and Banerjee, P, 2016, A comparative density functional theory and molecular dynamics simulation studies of the corrosion inhibitory action of two novel N-heterocyclic organic compounds along with a few others over steel surface, *J. Mol. Liq*., 215, 486–495.

[29] Becke, A.D., 1998, Density-functional exchange-energy approximation with correct asymptotic behavior, *Phys. Rev. A Gen. Phys.,* 38 (6), 3098–3100.

[30] Becke, A.D., 1993, Density-functional thermochemistry. I. The effect of the exchange-only gradient correction, *J. Chem. Phys.*, 98 (7), 5648–5652.

[31] Lee, C., Yang, W., and Parr, R.G., 1988, Development of the Colle-Salvetti correlation-energy formula into a functional of the electron density, *Phys. Rev. B: Condens. Matter.*, 37 (2), 785–789.

[32] Frisch, M.J., Trucks, G.W., Schlegel, H.B., Scuseria, G.E., Robb, M.A., Kudin, K.N., Strain, M.C., Farkas, O., Tomasi, J., Barone, V., Cossi,

M., Cammi, R., Mennucci, B., Pomelli, C., Adamo, C., Clifford, S., Ochterski, J., Petersson, G.A., Ayala, P.Y., Ui, Q., Morokuma, K., Malick, D.K., Rabuck, A.D., Raghavachari, K., Foresman, J.B., Cioslowski, J., Ortiz, J.V., Stefanov, B.B., Liu, G., Liashenko, A., Piskorz, P., Komaromi, I.R., Gomperts, R., Martin, L., Fox, D.J., Keith, T., Al-Laham, M.A., Peng, C.Y., Nanayakkara, A., Gonzalez, C., Challacombe, M.P., Gill, M.W., Johnson, B., Chen, W., Wong, M.W., Andres, J.L., Gonzalez, C., Head-Gordon, M., Replogle, E.S., and Pople. J.A., 2004, *Gaussian 03: Gaussian*, Inc. Wallingford., CT, 6492.

[33] Koopmans, T., 1934, Über die zuordnung von wellenfunktionen und eigenwerten zu den einzelnen elektronen eines atoms, *Physica*, 1 (1-6), 104–113.

[34] Foresman, J.B., and Frisch, A., 1995, *Exploring Chemistry with Electronic Structure Methods*, Gaussian, Inc., Pittsburg, PA (USA), 365.

[35] Pauling, L., 1960, *The Nature of the Chemical Bond*, Cornell University Press, Ithaca, New York.

[36] Pearson, R.G., 1990, Hard and soft acids and bases—the evolution of a chemical concept, *Coord. Chem. Rev.*, 100, 403–425.

[37] Sastri, V.S., and Perumareddi, J.R., 1997, Molecular orbital theoretical studies of some organic corrosion inhibitors, *Corros. Sci*., 53 (8), 617–622.

[38] Dewar, M.J.S., and Thiel, W., 1977, Ground states of molecules. 39. MNDO results for molecules containing hydrogen, carbon, nitrogen, and oxygen, *J. Am. Chem. Soc*., 99 (15), 4907–4917.

[39] Obayes, H.R., Alwan, G.H., Alobaidy, A.H.M.J., Al-Amiery, A.A., Kadhum, A.A.H., and Mohamad, A.B., 2014, Quantum chemical assessment of benzimidazole derivatives as corrosion inhibitors, *Chem. Cent. J*., 8, 21.

[40] Senet, P., 1997, Chemical hardnesses of atoms and molecules from frontier orbitals, *Chem. Phys. Lett*., 275 (5-6), 527–532.

[41] Ghosh, D.C., and Islam, N., 2011, Whether electronegativity and hardness are manifest two different descriptors of the one and the same fundamental property of atoms—A quest, *Int. J. Quantum Chem.*, 111 (1), 40–51.

[42] Sanderson, R.T., 1976, *Chemical Bond and Bond Energy*, Academic Press Inc., New York.

[43] Elshakre, M.E., Alalawy, H.H., Awad, M.I., and El-Anadouli, B.E., 2017, On the role of the electronic states of corrosion inhibitors: Quantum chemical-electrochemical correlation study on urea derivatives, *Corros. Sci*., 124, 121–130.

[44] Ramachandran, S., Tsai, B.L., Blanco, M., Chen, H., Tang, Y., and Goddard, W.A., 1997, Atomistic simulations of oleic imidazolines bound to ferric clusters, *J. Chem. Phys. A*, 101 (1), 83–89.

[45] Dewar, M.J.S., 1989, A critique of frontier orbital theory, *J. Mol. Struct. THEOCHEM*, 200, 301–323.

[46] Roque, J.M., Pandiyan, T., Cruz, J., and García-Ochoa, E., 2008, DFT and electrochemical studies of tris(benzimidazole-2-ylmethyl)amine as an efficient corrosion inhibitor for carbon steel surface, *Corros. Sci.*, 50 (3), 614–624.

[47] Turcio-Ortega, D., Pandiyan, T., Cruz, J., and García-Ochoa, E., 2007, Interaction of imidazoline compounds with Fe_n (n = 1-4 atoms) as a model for corrosion inhibition: DFT and electrochemical studies, *J. Phys. Chem. C*, 111 (27), 9853–9866.

[48] Fujimoto, H., and Inagaki, S., 1977, Orbital interaction and chemical bonds. Polarization in chemical reactions, *J. Am. Chem. Soc*., 99 (23), 7424–7432.